

**CASE FILE  
COPY**

**NATIONAL ADVISORY COMMITTEE  
FOR AERONAUTICS**

TECHNICAL NOTE

No. 1112

ANALYSIS OF PROPELLER EFFICIENCY LOSSES ASSOCIATED  
WITH HEATED-AIR THERMAL DE-ICING

By Blake W. Corson, Jr. and Julian D. Maynard

Langley Memorial Aeronautical Laboratory  
Langley Field, Va.



Washington  
July 1946

NATIONAL ADVISORY COMMITTEE FOR AERONAUTICS

---

TECHNICAL NOTE NO. 1112

---

ANALYSIS OF PROPELLER EFFICIENCY LOSSES ASSOCIATED  
WITH HEATED-AIR THERMAL DE-ICING

By Blake W. Corson, Jr. and Julian D. Maynard

SUMMARY

An analysis is made of the loss of efficiency associated with a heated-air thermal de-icing propeller both with and without internal flow. For the available data, measured efficiency losses are compared with the calculated losses and the agreement is found to be within the experimental accuracy of the data. The method presented may be used with reasonable accuracy to determine the net change in propeller efficiency due to the combined effects of the nozzle and internal flow if the characteristics of the propeller without nozzles are known.

INTRODUCTION

The problem of ice removal from an aircraft propeller in flight has been partly solved by each of several methods of propeller de-icing. These methods include the application of anti-icing pastes to the propeller blades, the dissolution of ice by alcohol or antifreeze fed to the blades by slinger ring and boots, the melting of ice from the blades by the use of electrically heated boots, and the melting of ice from the blades by heated-air thermal de-icing. By the last-mentioned method, which is particularly applicable to hollow metal blades, air is ducted from the free stream, heated either in a heat exchanger or by direct combustion, and passed through a gland into the rotating propeller where the heated internal flow heats and de-ices the propeller blades. The internal flow moves radially through the hollow blades and is discarded through nozzles at the blade tips into the propeller slipstream. All of these de-icing schemes entail some loss of propeller efficiency.

The efficiency losses associated with heated-air thermal de-icing were measured in tests of a two-blade hollow steel propeller in the Langley 16-foot high-speed tunnel. The primary purpose of the tests was to make a quick determination of the efficiency loss due to internal air flow. Because the temperature of the internal air flow was assumed to have little effect on the efficiency changes, the experimental propeller was made as simple as possible by dispensing with heat exchangers and by having the entire internal-flow system, inlet, ducts, and exit nozzles built into the propeller hub and blades. The results of the tests made with unheated internal flow are reported in reference 1. It is the purpose of this paper to attempt to express simply the efficiency loss as a function of the parameters which govern propeller operation and the internal air flow. The derived equations are correlated with the data presented in reference 1.

The change in propeller efficiency associated with heated-air thermal de-icing can be attributed to two effects; namely, the effect of the tip nozzle on the airfoil characteristics of the blade sections in the vicinity of the nozzle, and the effect of the internal flow on the power absorbed and the net thrust produced by the propeller. A complete theoretical evaluation of the efficiency change due to either of these effects is so involved as to be impractical. The magnitude of the efficiency changes, however, can be estimated with reasonable accuracy by introducing simplifying assumptions.

#### APPARATUS

A description of the dynamometer, propeller, and other apparatus used in the Langley 16-foot high-speed-tunnel tests of a thermal de-icing propeller is given in reference 1. A diagram of the internal-flow system tested in reference 1 and considered herein is given in figure 1 of this paper. A description of the apparatus is confined to the following list of propeller dimensions needed for use in applying the derived equations:

Number of blades . . . . .	2
Propeller diameter, feet . . . . .	12.208
Total nozzle exit area (2 blades), square foot . . . . .	0.00903
Radial location of center of nozzle ( $x = 0.95$ ), feet . . . . .	5.80

## ANALYSIS

## Effect of Nozzle Drag on Propeller Efficiency

Assumptions.- The problem of estimating the effect on propeller efficiency of a nozzle built into the blade tip can be approached most simply by assuming that only the drag of the blade sections in the region of the nozzle is affected. Although a chordwise section through the nozzle may have very poor lift and drag characteristics as an isolated airfoil, the same section used as a limited spanwise portion of an extensive airfoil will operate with approximately the same lift as the adjacent unaltered sections. The section drag, however, will be increased. This assumption is made in order that the derived equations may apply particularly to propellers to which nozzles are added at the very trailing edge of the blades.

Derivation.- Assume that the presence of a nozzle (without flow) creates an isolated drag on the propeller blade at radius  $r$ . Designate the total drag for all of the nozzles  $D_N$ . The drag acts in the direction of the resultant air velocity and may be resolved into two components, one a component of torque force in the plane of rotation, and the other a component of negative thrust. A diagram of the forces and velocities is given in figure 2. The nozzle drag reduces the propeller efficiency by increasing the power and reducing the thrust. The induced power loss, which is associated with blade section lift, is assumed not to change. If the propeller characteristics are known for the propeller without nozzles, the efficiency change due to the effect of nozzle drag on thrust and power can be expressed by differentiating the efficiency equation and treating the differentials as finite increments.

The symbols used in this paper are defined when they are introduced; a complete list of symbols is given in appendix A.

The efficiency equation is

$$\eta = \frac{C_T}{C_P} J \quad (1)$$

Differentiation gives

$$d\eta = \frac{J}{C_P} dC_T - \frac{\eta}{C_P} dC_P$$

$$\Delta\eta = \frac{J}{C_P} \Delta C_T - \frac{\eta}{C_P} \Delta C_P \quad (2)$$

where

- $C_T$  thrust coefficient  
 $C_P$  power coefficient  
 $\eta$  propeller efficiency  
 $J$  advance ratio

The nozzle drag acting at radius  $r$  is

$$D_N = \frac{1}{2} \rho W^2 A_N C_{D_N} \quad (3)$$

where

- $C_{D_N}$  nozzle external drag coefficient based on the total  
nozzle exit area  $A_N$   
 $W$  resultant air velocity  
 $\rho$  air density, slugs per cubic foot

Because the induced velocity at the propeller blade contributes only a very small component to the true resultant velocity, the resultant velocity can be evaluated with good accuracy as the vector sum of the forward velocity  $V$  and the rotational velocity as shown in figure 2

$$W = \sqrt{(\pi n D x)^2 + V^2} \quad (4)$$

where

D propeller diameter

n propeller rotational speed

x fraction of propeller tip radius

The component of the nozzle drag acting as negative thrust is

$$\Delta T = -D_N \left( \frac{V}{W} \right)$$

where  $\Delta T$  is the increment in propeller thrust. By use of equations (3) and (4), this equation becomes

$$\Delta T = -\frac{1}{2} \rho A_N C_{D_N} V \sqrt{(\pi n D x)^2 + V^2}$$

and in coefficient form is

$$\Delta C_T = -\frac{A_N}{D^2} \frac{C_{D_N}}{2} J \sqrt{(\pi x)^2 + J^2} \quad (5)$$

The component of the nozzle drag which creates torque is

$$\frac{\Delta Q}{r} = D_N \left( \frac{\pi n D x}{W} \right)$$

$$\Delta Q = r \frac{1}{2} \rho A_N C_{D_N} (\pi n D x) \sqrt{(\pi n D x)^2 + V^2}$$

$$\Delta P = 2\pi n \Delta Q$$

$$\Delta P = \rho n^3 D^5 \frac{A_N}{2D^2} C_{D_N} (\pi x)^2 \sqrt{(\pi x)^2 + J^2}$$

$$\Delta C_P = \frac{A_N}{D^2} \frac{C_{D_N}}{2} (\pi x)^2 \sqrt{(\pi x)^2 + J^2} \quad (6)$$

where

Q torque, foot-pounds

P power, foot-pounds per second

When the expressions for the increments of thrust and power coefficients (equations (5) and (6)) are substituted into equation (2), the efficiency loss due to nozzle drag is evaluated

$$\begin{aligned} \Delta\eta &= \frac{J}{C_P} \frac{-A_N}{D^2} \frac{C_{DN}}{2} J \sqrt{(\pi x)^2 + J^2} \\ &\quad - \frac{\eta}{C_P} \frac{A_N}{D^2} \frac{C_{DN}}{2} (\pi x)^2 \sqrt{(\pi x)^2 + J^2} \\ \Delta\eta &= -\frac{A_N}{D^2} \frac{C_{DN}}{2} \frac{\eta}{C_P} \sqrt{(\pi x)^2 + J^2} \left[ (\pi x)^2 + \frac{J^2}{\eta} \right] \quad (7) \end{aligned}$$

Application.- Equation (7) indicates that the efficiency loss due to propeller tip nozzle drag increases with increasing advance ratio and is directly proportional to the ratio of the efficiency to the power coefficient of the propeller without nozzles. For the thermal de-icing propeller of the present study, the power coefficient for maximum efficiency increased more rapidly with advance ratio than did the function of advance ratio (equation (7)) with the result that, at maximum efficiency, the loss due to the nozzles without flow decreased continuously within the range of advance ratio met in the tests. For want of better nozzle-drag data, the nozzle-drag coefficient was assumed to be the same as that for a flat plate and the efficiency loss due to the nozzles without internal flow was computed. The values of advance ratio, power coefficient, and efficiency at peak efficiency for the normal propeller

were taken from figures 13 and 14 of reference 1 and are listed in table I with the computed and measured values of efficiency loss. The efficiency loss due to the nozzles without internal flow is also shown in figure 3 as a function of advance ratio. The trend with advance ratio of the measured loss is similar to that indicated in equation (7).

The foregoing computations were for operation at peak efficiency. The efficiency loss due to the nozzles without internal flow for any condition of operation should not be much different from that shown in figure 3. The most common conditions of propeller operation are at values of advance ratio less than that for peak efficiency: in this range the power coefficient is increased and equation (7) indicates that the efficiency loss is less than for operation at peak efficiency. Of less interest is operation at values of advance ratio greater than the values for peak efficiency for which both the power coefficient and the efficiency decrease with increasing advance ratio, with the result that the efficiency loss is seldom much greater than that shown in figure 3 and is generally less.

#### Effect of Internal Flow on Propeller Efficiency

Assumptions.- The same approach is used in estimating the effect of the internal flow on the efficiency of a heated-air thermal de-icing propeller as was followed in estimating the effect of the nozzle drag alone. The motion of the internal flow through the propeller is accompanied by finite changes to the propeller thrust and power from which the efficiency change can be computed. There are four increments of thrust and power associated with the internal flow that affect the propeller efficiency. These increments are: (1) a negative thrust incurred by inducting the internal flow from the free-air stream and arresting its axial motion with respect to the propeller, (2) a power increase required for the centrifugal pumping of the internal flow by the propeller, (3) a positive thrust component of the jet reaction contingent upon the proper ejection of the internal flow through the tip nozzle, and (4) an increment of useful power from the torque component of the jet reaction.

A discussion of the influence of the thermodynamic processes affecting the internal flow will be reserved for a subsequent section of this paper. It is conceivable that a small amount of engine shaft power can be dissipated from any propeller as heat. The temperature rise of a body immersed in a high-speed air flow is discussed in reference 2, which maintains that, because of complete arrest of the flow both at the stagnation point and in the boundary layer, the equilibrium temperature of the entire body is the stagnation temperature. The various sections of a propeller blade operate at different airspeeds; the tip sections operate at the highest speed and the shank sections at the lowest. Consequently, a radial temperature gradient exists and causes a flow of heat from the blade tip toward the shank. (See reference 3.) As the shank becomes hotter than its stagnation temperature, it is cooled by the air flow. Thus, indirectly, a small amount of shaft energy supplied by the engine is dissipated through the propeller as heat.

In the case of the heated-air thermal de-icing propeller, the external-flow temperature conditions are the same as for a normal propeller, and for ideal internal flow, the stagnation temperatures of air within the blade will be identical at all radii with the external stagnation temperatures. This equality exists because the stagnation temperature of the internal flow at the inner surface of the blade is determined by the combined effects of the free-stream velocity possessed by the internal flow before its induction, and its radial velocity, manifest as total pressure rise, which is always equivalent to the tangential velocity. Hence, in the ideal case without heat transfer the total pressure of the internal flow at any radius equals that of the external flow; the internal and external stagnation temperatures are therefore equal, and the dissipation of engine power as heat is no greater for a heated-air thermal de-icing propeller than for a conventional propeller. The effect of the internal flow on the propeller efficiency is determined almost entirely by the exchange of mechanical energy between the internal flow and the propeller.

Internal-flow induction, negative thrust.- The induction of the internal flow from the free-air stream into the propeller is accompanied by an inescapable

negative thrust proportional to the product of the internal mass flow and the change of axial velocity with respect to the propeller. This relation holds regardless of the manner in which the air is taken from the free stream and ducted into the propeller. The processes involved in handling the internal air flow affect the total pressure of the internal flow which, as will be shown, affects the mass flow and the exit velocity but not the negative thrust. The negative thrust exerted by the internal air flow upon the propeller or airplane at induction is

$$\Delta T = -mV \quad (8)$$

where

$m$  internal mass flow, slugs per second

$V$  velocity of advance, feet per second

By expressing the mass flow in coefficient form, equation (8) becomes

$$\Delta T = -m_c \rho A_N n D V$$

$$\Delta C_T = -\frac{A_N}{D^2} m_c J \quad (9)$$

where, by definition,

$$m_c = \frac{m}{\rho A_N n D}$$

Significance of mass-flow coefficient.- A simple interpretation of the mass-flow coefficient is that the coefficient expresses a relation of the velocity of flow from the nozzle to the rotational tip speed of the propeller. If the density of the internal flow at the

nozzle is equal to that of the atmosphere in which the propeller is operating, a value of the mass-flow coefficient equal to  $\pi$  indicates that the velocity of efflux from the nozzle is equal to the propeller rotational tip speed. The mass-flow coefficient could have been so defined as to equal unity or any other arbitrary value for the specified condition, but the definition given is in keeping with conventional propeller coefficients.

Centrifugal pumping power.- Consideration of the motion of an unrestrained particle under the action of centrifugal force shows that at all times the tangential acceleration of the particle is equal to the radial acceleration; velocity changes and the corresponding kinetic-energy changes resulting from the two accelerations must be equal. Energy per unit mass imparted to the particle by the tangential motion must always be kinetic energy equal to one-half the tangential velocity squared. Likewise, for an unrestrained particle, the kinetic energy due to the radial motion is equal to that for the tangential motion. In the case of fluid motion under centrifugal action, the particles composing the flow are usually partly restrained, and the energy, which for the individual particle was radial kinetic energy, will appear as a combination of kinetic energy, pressure energy, and (for a gas) heat due to compression. By the law of the conservation of energy, however, the total energy per slug of mass flow imparted by the propeller to the internal flow at a point immediately ahead of the tip nozzle is equal to twice the kinetic energy due to the tangential velocity; that is

$$\text{Energy per second} = m(\omega r)^2$$

where

$\omega$  angular velocity, radians per second

The energy per second is the centrifugal pumping power, which may be expressed as follows:

$$\Delta P = m(\pi n D x)^2 \quad (10)$$

A more rigorous derivation of the relation expressed by equation (10) is given in reference 4, which shows that, when shaft power is not dissipated as heat, the power required for a centrifugal blower depends only on the mass flow and the tangential velocity imparted to the flow.

By expressing the mass flow in coefficient form, equation (10) may be rewritten

$$\Delta P = m_c \rho A_N n D (\pi n D x)^2$$

$$\Delta C_P = \frac{A_N}{D^2} m_c (\pi x)^2 \quad (11)$$

Equation (11) expresses the increment of power coefficient required for pumping the internal flow through the propeller.

The foregoing considerations of the effect of the internal flow on the thrust and power have shown the effects to be detrimental. The change of direction of the internal flow, moving with free-stream velocity, from an axial to a radial motion was shown to create the negative thrust expressed by equation (9). The centrifugal pumping action of the hollow-blade propeller working on the internal flow was shown to increase the power absorbed by the propeller in an amount expressed by equation (11). Neither of these processes necessarily represents a complete loss because the energy involved is merely transferred to the internal flow. The negative thrust due to stopping the air cannot be avoided, but, with efficient diffusion and ducting, the air will retain its energy either as kinetic or pressure energy which can be reconverted into positive thrust on being ejected from the tip nozzle. Likewise, the energy imparted to the internal flow in the centrifugal pumping process can be reconverted into power tending to drive the propeller.

Tip-nozzle jet propulsion.- For simplicity, the analysis of the jet-propulsion effect of the propeller tip nozzle will be idealized as was the treatment of the

negative thrust and centrifugal pumping effects. The internal flow is assumed to move in a purely radial direction within the blade until it reaches the vicinity of the tip nozzle where it is turned through a right angle. In the ideal case, the internal flow is ejected from the blade through the tip nozzle in a direction normal to the radius and parallel to the resultant velocity of the external flow at the station of the tip nozzle. (See fig. 4.) The foregoing assumption can be true for only one value of advance ratio for each blade angle, but for controllable-pitch propeller operation the direction of the internal-flow jet from the tip nozzle would never deviate more than a few degrees from the direction of the external resultant air flow.

The reaction due to ejection of the internal flow from the tip nozzle is a force tentatively normal to the radius tending to drive the blade section at the nozzle along its helical path. In practice, the nozzle will hardly be completely effective in directing all of the internal flow downstream along the helical path. If means exist for estimating the nozzle effectiveness, here designated as  $\epsilon$ , the jet velocity  $V_N$  can be multiplied by this factor to yield a better estimate of the jet reaction than by merely assuming perfect nozzle effectiveness. The nozzle effectiveness is not jet efficiency but may be regarded mainly as the cosine of the acute angle between the mean direction of flow from the nozzle and the helical path of the nozzle. Because the change of velocity of the internal flow with respect to the blade is the jet velocity, the force on the blade due to the jet reaction  $F_N$  is the product of mass flow, jet velocity, and nozzle effectiveness; therefore,

$$F_N = mV_N \epsilon \quad (12)$$

Continuity of the mass flow must be preserved, hence the jet velocity can be expressed in terms of the mass flow, thus

$$m = m_c \rho_A n D = \rho_N A_N V_N$$

$$V_N = \left( \frac{\rho_c}{\rho_N} \right) m_c n D \quad (13)$$

If the mass flow in equation (12) is expressed in coefficient form and equation (13) is used for the jet velocity, equation (12) becomes

$$F_N = \rho A_N \left( \frac{\rho}{\rho_N} \right) (nD)^2 \epsilon m_c^2 \quad (14)$$

The diagram (fig. 4) shows that the component of the jet force, which acts as positive thrust, is

$$\Delta T = F_N \times \frac{V}{W} \quad (15)$$

The substitution in equation (15) of equations (4) and (14) for  $W$  and  $F_N$ , respectively, results in the following expression for the positive thrust increment

$$\Delta T = \rho A_N \left( \frac{\rho}{\rho_N} \right) (nD)^2 \epsilon m_c^2 \frac{V}{\sqrt{(\pi n D x)^2 + V^2}}$$

then

$$\Delta C_T = \frac{A_N}{D^2} \left( \frac{\rho}{\rho_N} \right) \epsilon m_c^2 \frac{J}{\sqrt{(\pi x)^2 + J^2}} \quad (16)$$

The component of the jet force, which acts normal to the radius and in the plane of rotation to produce a driving torque, regarded as negative because propeller torque is positive, is

$$\Delta Q = -F_N r \frac{\pi n D x}{W}$$

When equations (4) and (14) are substituted for  $W$  and  $F_N$ , respectively, the foregoing expression for torque increment becomes

$$\Delta Q = -\rho A_N \left( \frac{\rho}{\rho_N} \right) (nD)^2 \epsilon m_c^2 r \frac{\pi n D x}{\sqrt{(\pi n D x)^2 + V^2}}$$

$$\Delta P = -2\pi n \Delta Q$$

$$\Delta P = -2\pi n \rho A_N \left( \frac{\rho}{\rho_N} \right) (nD)^2 m_c^2 \epsilon r \frac{\pi n D x}{\sqrt{(\pi n D x)^2 + V^2}}$$

$$\Delta C_P = -\frac{A_N}{D^2} \left( \frac{\rho}{\rho_N} \right) m_c^2 \epsilon \frac{(\pi x)^2}{\sqrt{(\pi x)^2 + J^2}} \quad (17)$$

Net thrust increment.- The total effect of the internal flow on the thrust coefficient is the combined negative thrust incurred during induction and positive thrust obtained at rejection, equations (9) and (16), respectively; thus

$$\Delta C_T = \frac{A_N}{D^2} \left( \frac{\rho}{\rho_N} \right) m_c^2 \epsilon \frac{J}{\sqrt{(\pi x)^2 + J^2}} - \frac{A_N}{D^2} m_c J$$

$$\Delta C_T = \frac{A_N}{D^2} m_c J \left[ \left( \frac{\rho}{\rho_N} \right) \frac{m_c \epsilon}{\sqrt{(\pi x)^2 + J^2}} - 1 \right] \quad (18)$$

Net power increment.- The total effect of the internal flow on the power coefficient is the net effect of the pumping power and of the propulsive power obtained from the tip jet, expressed by equations (11) and (17), respectively; therefore

$$\Delta C_P = \frac{A_N}{D^2} (\pi x)^2 m_c - \frac{A_N}{D^2} \left( \frac{\rho}{\rho_N} \right) \epsilon m_c^2 \frac{(\pi x)^2}{\sqrt{(\pi x)^2 + J^2}}$$

$$\Delta C_P = \frac{A_N}{D^2} (\pi x)^2 m_c \left[ 1 - \left( \frac{\rho}{\rho_N} \right) \frac{m_c \epsilon}{\sqrt{(\pi x)^2 + J^2}} \right] \quad (19)$$

Effect of internal flow on efficiency.- The same procedure that was followed in the case of the nozzles without flow can be used to determine the effect of the internal flow on the propeller efficiency. The efficiency change due to the internal flow can be evaluated by substituting the finite increments of thrust and power coefficient, equations (18) and (19), into equation (2), thus

$$\Delta \eta = \frac{J}{C_P} \Delta C_T - \frac{\eta}{C_P} \Delta C_P \quad (\text{Equation (2)})$$

$$\Delta \eta = \frac{J}{C_P} \frac{A_N}{D^2} m_c J \left[ \left( \frac{\rho}{\rho_N} \right) \frac{m_c \epsilon}{\sqrt{(\pi x)^2 + J^2}} - 1 \right]$$

$$- \frac{\eta}{C_P} \frac{A_N}{D^2} (\pi x)^2 m_c \left[ 1 - \left( \frac{\rho}{\rho_N} \right) \frac{m_c \epsilon}{\sqrt{(\pi x)^2 + J^2}} \right]$$

$$\Delta \eta = \frac{A_N}{D^2} \frac{\eta}{C_P} m_c \left[ \left( \frac{\rho}{\rho_N} \right) \frac{m_c \epsilon}{\sqrt{(\pi x)^2 + J^2}} - 1 \right] \left[ (\pi x)^2 + \frac{J^2}{\eta} \right] \quad (20)$$

Equation (20) shows that the change of propeller efficiency associated with the internal flow varies with mass flow coefficient, nozzle area, nozzle effectiveness, and density ratio, as well as with the usual propeller characteristics. Whether the efficiency changes represent a loss depends upon the magnitude of the term

$$\frac{\rho}{\rho_N} \frac{m_c \epsilon}{\sqrt{(\pi x)^2 + J^2}}$$

When no pressure is applied to the internal flow except the impact pressure due to airspeed and the centrifugal pressure due to propeller rotation, the foregoing term can never be greater than unity as can be shown by use of equation (27) and the definition of nozzle effectiveness. Hence the quantity in the first brackets of equation (20) must be negative and the efficiency change a loss. If pressure is applied to the internal flow by a pump or blower, the mass-flow coefficient can be made sufficiently large to make the efficiency change calculated from equation (20) positive. This positive efficiency change would mean only that, due to the propulsive effect of the tip nozzles, the thrust-power output of the propeller had been increased; the net efficiency change, when the additional power supplied to the pump or blower is accounted for, would most likely still be negative (except in some cases when heat is added to the internal flow under pressure).

Application.- The values of efficiency loss due to the internal flow calculated from equation (20) are of the same order of magnitude as the loss indicated by the tests of reference 1. Values of advance ratio, power coefficient, and efficiency at maximum efficiency for the propeller with nozzles but without flow are listed in table II, corresponding values of mass-flow coefficient and density ratio are listed for the propeller with internal flow. The density ratio, which applies only to these data, was obtained by the procedure outlined in appendix B and discussed in the section dealing with internal drag. Inasmuch as the flow traces at the nozzles observed at the termination of the tests indicated

some radial flow, a nozzle effectiveness of  $\epsilon = 0.75$  was assumed. The computed and measured values of efficiency loss due to internal flow are compared in table II and are shown graphically in figure (5).

### Combined Losses

The net loss of propeller efficiency associated with the internal air flow (unheated) can be expressed by the addition of the individual losses due to the nozzle drag and the internal flow, equations (7) and (20), thus

$$\Delta\eta = \frac{A_N}{D^2} \frac{\eta}{C_P} \left[ (\pi x)^2 + \frac{J^2}{\eta} \right] \left\{ m_c \left[ \frac{\rho}{\rho_N} \frac{m_c \epsilon}{\sqrt{(\pi x)^2 + J^2}} - 1 \right] - \frac{C_{DN}}{2} \sqrt{(\pi x)^2 + J^2} \right\} \quad (21)$$

In table III the values of advance ratio, power coefficient, and efficiency at peak efficiency are listed for the normal propeller; and the values of mass-flow coefficient and density ratio (appendix B) are given for the propeller with internal flow. Also in table III the measured loss of efficiency due to the combined effect of the tip nozzles and internal flow is compared with the corresponding loss computed from equation (21); a graphical comparison is given in figure 6.

Inasmuch as the net accuracy claimed for the measurements of reference 1 is only  $\pm 1$  percent, the agreement of the calculated efficiency losses with the measured values shown in figures (3), (5), and (6) is unexpectedly good. Only one measured value falls outside the limit of accuracy and most of the measured values are within a few tenths of a percent of the corresponding calculated value. Inasmuch as admission of the internal flow was expected to have caused a reduction of the nozzle drag, the good agreement of the calculated with the measured results may be due to a fortunate selection of the assumed values for nozzle-drag coefficient and for

nozzle effectiveness. The assumed values both of nozzle-drag coefficient (with internal flow) and nozzle effectiveness are probably too large, but because their effects are compensating, the calculated efficiency loss agrees well with the measured values. One encouraging indication of the validity of the derived equations, however, is that in all cases the trend of the data follows that of the calculated curve; that is, the efficiency loss at peak efficiency associated with the nozzle drag and internal flow decreases with increasing advance ratio within the range of advance ratio of the tests.

### Internal Loss

Assumptions.- Thus far in the discussion of the heated-air thermal de-icing propeller, energy losses in the internal flow have not been considered. Changes in the propeller thrust and power coefficients and efficiency have been expressed conveniently in terms of the mass-flow coefficient. In the part of the analysis that follows, a relation between the internal mass-flow coefficient and the internal loss is developed. The derivation is based entirely on kinetic-energy changes in the internal flow. The static pressure at the nozzle exit is assumed to be the same as that of the free-air stream. Compressibility of the air is not accounted for in the derivation because an accurate and consistent estimation of the static-pressure variation in the internal flow is not feasible. The assumptions upon which the derivation is based make the equation adaptable to use with the data presented in reference 1, in which density changes between the free-stream air and the internal flow at the nozzle were small because no heat was added to the internal flow. An attempt is made, however, to preserve the validity of the expression for cases which involve considerable density change by including in the equations the factor which expresses density ratio. The inclusion of the density-ratio factor is believed to make the incompressible flow equations good approximations for the cases in which heat is added to the internal flow or for the cases in which the internal pressure loss is converted to heat.

Internal pressure loss.- For this analysis the internal loss is regarded as the combined resistance offered to the internal flow by the skin friction of

the internal system; by turbulence introduced in the flow by abrupt turns, sharp corners, poor nozzle shape, and inefficient diffusion; and by changes in flow pattern with rotational speed typical of centrifugal blowers. One concept of the internal energy loss is that of an equivalent pressure loss acting on the volume flow at the nozzle, as

$$\text{Internal energy loss per second} = \Delta p_f A_N V_N$$

An additional energy equal to the kinetic energy of the internal flow at the nozzle leaves the system each second with the ejected internal flow. The net power required to move the internal flow is

$$P_R = \Delta p_f A_N V_N + \frac{m V_N^2}{2} \quad (22)$$

Pressure available.- The pressure available for moving the internal flow through the propeller is derived from three sources: the impact pressure of the free-air stream, the centrifugal pumping pressure, and the aerodynamic suction due to the low-pressure field surrounding the nozzle exterior. The pressure at the nozzle exit depends upon the location of the nozzle on the blade section and upon the angle of attack at which the section is operating. The effect of low pressure at the nozzle exit in moving the internal flow was found in the tests of reference 1 to be very small and will not be considered in this analysis. That is, the static pressure at the nozzle is assumed to be the atmospheric pressure in which the propeller is operating.

If care is exercised in the induction of the internal flow, the kinetic energy of the free-air stream relative to the airplane can be made to furnish a part of the motive power for the internal flow. At a point upstream of the airplane the internal flow before its induction has a velocity  $V$  with respect to the airplane. The

kinetic energy per second entering with the internal flow, which can be used for pumping the flow through the internal system, is

$$\text{Energy per second} = \frac{m}{2} v^2$$

In the discussion of the power expended in pumping the internal flow through the propeller centrifugally, it was shown that one-half of the power appeared as an increase in the total pressure of the internal flow (with respect to the blade), from equation (10)

$$\text{Energy per second} = \frac{m}{2} (\pi n D x)^2$$

The net power available for moving the internal flow is

$$P_A = \frac{m}{2} \left[ (\pi x)^2 + J^2 \right] (nD)^2 \quad (23)$$

The power available can also be regarded as the product of volume flow at the nozzle and an equivalent pressure available

$$P_A = \Delta p_A A_N V_N$$

By combining the two foregoing equations, the equivalent pressure available is expressed in terms of measurable quantities

$$\Delta p_A = \frac{m}{2 A_N V_N} \left[ (\pi x)^2 + J^2 \right] (nD)^2$$

or, by use of the definition of mass flow,

$$\Delta p_A = \frac{\rho_N}{2} [(\pi x)^2 + J^2] (nD)^2 \quad (24)$$

Relation between  $\Delta p_f$  and  $m_c$ . - When the motion of the internal flow reaches a steady state, the energies required and available for maintaining the flow are in equilibrium and the expression for power required in equation (22) can be replaced by that for power available, equation (23); thus

$$\Delta p_f A_N V_N + \frac{m V_N^2}{2} = \frac{m}{2} [(\pi x)^2 + J^2] (nD)^2$$

or

$$\frac{\Delta p_f}{q_N} = \frac{\frac{\rho_N}{2} [(\pi x)^2 + J^2] (nD)^2}{q_N} - 1 \quad (25)$$

where

$$q_N = \frac{1}{2} \rho_N V_N^2$$

The dynamic pressure at the nozzle may be expressed in terms of the mass-flow coefficient as

$$q_N = \frac{\rho_N}{2} \left( \frac{\rho}{\rho_N} m_c nD \right)^2$$

Upon substitution of this expression for  $q_N$  into equation (25), the internal pressure loss is expressed in terms of nondimensional propeller parameters and a density ratio,

$$\frac{\Delta p_f}{q_N} = \left(\frac{\rho_N}{\rho}\right)^2 \frac{[(\pi x)^2 + J^2]}{m_c^2} - 1 \quad (26)$$

A regrouping of the terms in equation (26) provides a convenient relation between mass-flow coefficient and internal pressure loss

$$m_c = \left(\frac{\rho_N}{\rho}\right) \sqrt{\frac{(\pi x)^2 + J^2}{\frac{\Delta p_f}{q_N} + 1}} \quad (27)$$

Throughout this analysis the internal pressure loss is expressed as a ratio to the dynamic pressure at the nozzle. Another relation that may be useful is the ratio of internal pressure loss to the pressure available, which for the equilibrium condition is shown by the following identity:

$$\frac{\Delta p_f}{\Delta p_A} = \frac{\frac{\Delta p_f}{q_N}}{\frac{\Delta p_f}{q_N} + 1} \quad (28)$$

Determination of  $\Delta p_f/q_N$  from bench tests.- A foreknowledge of the value of the internal pressure loss for a blade and nozzle combination is useful for estimating probable efficiency losses to be encountered with a proposed propeller design. Equation (26) provides a basis

for the experimental determination of the internal pressure loss from bench tests. A setup might be made in any of a number of ways, but a simple arrangement is to surround the tip nozzle or nozzles with a low-pressure chamber to induce an internal flow through the propeller. A metering orifice at the entrance to the system, where total pressure is atmospheric, measures the impact pressure as the difference between atmospheric pressure and the static pressure  $p_0$  in the orifice. From this measurement, with the atmospheric pressure and the metering-orifice area known, both the internal mass flow and the dynamic pressure  $q$  of the flow at the entrance can be calculated. The only other measurements needed are the static pressure and temperature at the nozzle, by which the density of the air at the nozzle may be determined, and the flow area at the nozzle  $A_N$ . In this case the rotational speed is zero and equation (26) can be reduced to the form:

$$\frac{\Delta p_f}{q_N} = \frac{2(\rho_N A_N)^2}{\rho} \frac{q}{m^2} - 1 \quad (29)$$

A procedure for calculating the internal mass flow from knowledge of the ratio of impact pressure to atmospheric pressure  $\Delta p/p_a$  is given in reference 1; the relation between  $q/p_a$  and  $\Delta p/p_a$  is shown in figure 7 of the present paper.

The ratio  $\Delta p_f/q_N$  is not a true coefficient by which the internal pressure loss may be expressed. The ratio applies only to a given combination of propeller blade and tip nozzle and, for a given blade, will change when the nozzle area is changed. The ratio will also change with rotational speed unless proportionate changes occur in both internal pressure loss and dynamic pressure at the nozzle.

Calculation of nozzle area.- If the condition of equilibrium between the power required and that available for moving the internal flow is again considered,

equation (22) can be used to obtain an expression for nozzle area

$$\Delta p_A A_N V_N = \Delta p_f A_N V_N + \frac{m V_N^2}{2}$$

$$\Delta p_A - \Delta p_f = \frac{m V_N}{2 A_N} = \frac{m^2}{2 \rho_N A_N^2}$$

$$A_N = \sqrt{\frac{m^2}{2 \rho_N (\Delta p_A - \Delta p_f)}} \quad (30)$$

When the required mass flow and heat exchanged are known and when the internal pressure loss  $\Delta p_f$  has been estimated (bench tests), the density of the air at the nozzle can be calculated from the following equation, which is derived in appendix C:

$$\rho_N = \frac{\rho - \frac{\Delta p_f}{778 c_p t}}{1 + \frac{H_I - H_D}{m c_p t}} \quad (31)$$

where  $H_I$  is the rate (Btu per second) at which heat contained in the internal flow enters the propeller and  $H_D$  the rate at which heat is dissipated through the propeller blade surface for de-icing. The pressure available can then be calculated from equation (24) and all quantities necessary for the calculation of nozzle area from equation (30) are known. Equation (30) furnishes a means for the calculation of the nozzle

area necessary for the rejection of a given internal mass flow. By making the nozzle the section of greatest restriction in the internal-flow system, velocities elsewhere in the system may be made as small as feasible and the internal losses may be reduced to the practical minimum. Because the pressure available is fixed by the operating conditions, the advantage of achieving a minimum of internal loss is demonstrated by equation (30), which shows that the minimum nozzle area is obtained when the internal loss is reduced to a practical minimum.

Effect of internal loss on efficiency.- The loss of propeller efficiency associated with the internal flow has been expressed by equation (20) in terms of the mass flow coefficient and correlated with the measured values of reference 1. When equation (27) is substituted for the mass-flow coefficient in equation (20), the loss of propeller efficiency due to the internal flow is shown directly related to the internal pressure loss, thus

$$\Delta\eta = \frac{A_N}{D^2} \frac{\eta}{C_P} \frac{\rho_N}{\rho} \sqrt{\frac{(\pi x)^2 + J^2}{\frac{\Delta p_f}{q_N} + 1}} \left[ \frac{\epsilon}{\left(\frac{\Delta p_f}{q_N}\right) + 1} - 1 \right] \left[ (\pi x)^2 + \frac{J^2}{\eta} \right] \quad (32)$$

The first bracketed term in equation (32) shows that the efficiency loss increases as the internal pressure loss increases and as the nozzle effectiveness decreases. With perfect nozzle effectiveness and no internal pressure loss, there is no loss of efficiency associated with the internal flow. Equation (32) illustrates the importance of reducing the internal pressure loss and of designing the tip nozzle for greatest effectiveness in producing jet propulsion.

#### DISCUSSION

Elimination of density ratio from equation (26).- The propeller test data in reference 1, for the propeller with internal flow, present measured values of all quantities in equation (26) necessary for calculating the internal pressure loss, except the density of the flow at the nozzle. An estimate of  $\Delta p_f/q_N$  with a density ratio of unity assumed indicates that the internal loss consumes more than half of the energy available for moving

the internal flow. Inasmuch as the mechanical energy loss appears as heat in the internal flow, the air density at the nozzle must be reduced to an extent that cannot be ignored. In appendix B an expression, equation (33), is derived for calculating  $\Delta p_f/q_N$  in which the density change is regarded as dependent upon  $\Delta p_f/q_N$

$$\sqrt{\frac{(\pi x)^2 + J^2}{\left(\frac{\Delta p_f}{q_N} + 1\right) m_c^2}} = 1 + \frac{(nD)^2}{2 \times 778 c_p t} \left( \frac{\frac{\Delta p_f}{q_N}}{\frac{\Delta p_f}{q_N} + 1} \right) [(\pi x)^2 + J^2] \quad (33)$$

Equation (33) is regarded as applicable only for internal flow systems similar to that treated in reference 1. A solution of equation (33) for  $\Delta p_f/q_N$  is given in appendix B.

Data selected from reference 1 for several different operating conditions are listed in table IV with the corresponding values of  $\Delta p_f/q_N$  computed from equation (33). Also listed are the computed density ratio and the nominal angle of attack of the propeller blade sections at the nozzle station.

Effect of static pressure at nozzle exit. - It was assumed in deriving the expression for  $\Delta p_f/q_N$  that the static pressure at the nozzle exit was equal to the atmospheric pressure in which the propeller was operating. If the exit pressure were appreciably lower than the atmospheric pressure, the calculated value of  $\Delta p_f/q_N$  would be too small. At low values of advance ratio (large angle of attack), it might be expected that greater nozzle-exit suction would exist than for high values of advance ratio (small angle of attack). If this effect were appreciable, the aerodynamic suction at the exit for low values of  $J$  would be manifest as lower internal loss. The measured variation of  $\Delta p_f/q_N$  with nominal angle of attack, at fixed blade angle and rotational speed, is shown in table IV to be small and inconsistent,

which indicates that the static pressure at the nozzle exit did not vary appreciably from atmospheric pressure and that the assumption made in this regard is justified.

Effect of rotational speed.- Average values of  $\Delta p_f/q_N$  at several values of rotational speed are shown in figure 8; the average variation with rotational speed of the density ratio (applicable to the data of reference 1) is also shown in this figure. The internal pressure loss coefficient  $\Delta p_f/q_N$  (which is proportional to skin friction and turbulence losses) increases with increasing rotational speed. Because the Reynolds number of the internal flow increased with rotational speed, the variation of  $\Delta p_f/q_N$  with rotational speed might be explained as a viscous effect. Another possible cause for the variation of  $\Delta p_f/q_N$  is compressibility of the air, but drag losses, in general, change abruptly when the cause is a compressibility effect. It is more probable, however, that the increase of  $\Delta p_f/q_N$  with rotational speed is due to the ineffectiveness of the hollow propeller blades as a centrifugal impeller.

The curve shown in figure 8 is for data taken during propeller tests at the constant rotational speed that is regarded as the best presented in reference 1. Random points at various rotational speeds from tests at constant advance ratio are also plotted on this figure, but are regarded as inferior data.

Jet efficiency.- The efficiency with which the jet from the tip nozzle propels the blade section at the nozzle station along its helical path is the ratio of thrust work (along the helical path) to the sum of thrust work and residual kinetic energy in the jet:

$$\eta_N = \frac{m\epsilon V_N W}{m\epsilon V_N W + \frac{1}{2}m(W - V_N)^2}$$

which upon simplification becomes

$$\eta_N = \frac{1}{1 + \frac{W}{2\epsilon V_N} \left(1 - \frac{V_N}{W}\right)^2} \quad (34)$$

Equation (34) shows that the propulsive efficiency of the tip jets is greatest when perfect nozzle effectiveness ( $\epsilon = 1.0$ ) is achieved and when the jet velocity equals the section resultant velocity; that is, when the ejected internal flow remains motionless with respect to the atmosphere. The propulsive efficiency of the nozzle decreases when the jet velocity  $V_N$  is either less than the resultant velocity, as is the case for the tests of reference 1, or greater, as might result from applying considerable pressure to move the internal flow. If nozzles were formed by cutting off a portion of the propeller tips so that the internal flow would be ejected radially, all the energy used in pumping the internal flow through the blades would be lost; the nozzle effectiveness would be zero, and the jet-propulsive efficiency as shown by equation (34) would be zero.

By use of equations (4) and (13) to express  $W$  and  $V_N$ , respectively, the jet efficiency can be expressed in terms of the mass-flow coefficient

$$\eta_N = \frac{1}{1 + \frac{\sqrt{(\pi x)^2 + J^2}}{2\epsilon \frac{\rho}{\rho_N} m_c} \left[ 1 - \frac{\frac{\rho}{\rho_N} m_c}{\sqrt{(\pi x)^2 + J^2}} \right]^2} \quad (35)$$

or in terms of the internal pressure loss, from equation (27),

$$\eta_N = \frac{1}{1 + \frac{\left[ \sqrt{\left( \frac{\Delta p_f}{q_N} \right) + 1} - 1 \right]^2}{2\epsilon \sqrt{\left( \frac{\Delta p_f}{q_N} \right) + 1}}} \quad (36)$$

Equation (35) is generally applicable, but, because  $(\Delta p_f/q_N)$  is defined for the case when the pumping pressure for the internal flow is supplied only by the airspeed and propeller rotation, equation (36) does not apply when additional pressure is supplied to the internal flow by pump or blower. Equation (36) further emphasizes the desirability of reducing the internal loss to a minimum.

Effect of heat. - At least three general effects of heat added to the internal flow will probably be felt. The first, an aerodynamic effect of the added heat, is that an increase in pressure will be required to force a given mass flow through the internal system; or, with no change in the pumping facility, the mass flow will be less for the heated condition than for the cold. This phenomenon is the same as that encountered with heat exchangers in general and exists whether the heat is added through a heat exchanger or by direct combustion in the internal flow. The relation between the increased pressure required and the heat added is discussed in reference 5. A second effect is inverse to that just described; that is, in the region where heat is being dissipated through the surface of the propeller blade to perform the de-icing task, less forcing pressure is required to move the internal flow when heated than would be required to move a cold internal flow from which heat is not being dissipated. The two effects are partly compensating but, because the internal flow must be maintained at a fairly high temperature up to the time it is rejected through the tip nozzles, the net effect of the heating and cooling is either to require a net increase in forcing pressure, or to result in a slightly diminished mass flow. The third effect is that the elevated temperature at the nozzles results in a reduced density and increased velocity of the flow from the nozzles.

One scheme worthy of consideration in connection with heating the internal flow is the conversion of some of the heat into mechanical energy. The internal-flow system of a thermal de-icing propeller is basically similar to that of jet-propulsion engines; air taken from the free stream into the internal system is retarded with pressure increase, heated, accelerated, and rejected with an increased momentum which produces thrust. With a heated-air thermal de-icing propeller, it would be advantageous to add the heat at the point where the

internal flow is under greatest static pressure even though the elevated pressure is no more than total pressure. The result would be an increase in the nozzle jet-propulsive effect and therefore at least a smaller loss in the propeller efficiency.

### CONCLUSIONS

An analysis of the forces acting on a heated-air thermal de-icing propeller with and without internal flow indicates the following conclusions:

1. The nozzle exit area should be the smallest that will discharge an internal flow sufficient for de-icing the propeller, for the following reasons:

(a) The efficiency loss for the propeller without internal flow is proportional to the nozzle exit area and nozzle drag coefficient.

(b) By making the nozzle the section of greatest restriction in the internal-flow system, velocities elsewhere in the system may be made as small as feasible and the internal losses may be reduced to a practical minimum.

(c) A further result is the highest attainable discharge velocity of the internal flow and consequent greatest propulsive effect from the nozzle jets.

2. The efficiency loss that accompanies the admission of the internal flow increases with:

(a) The internal-mass flow.

(b) The product of internal-mass flow and the effectiveness of the nozzle in ejecting the internal flow downstream along the helical path of the nozzle.

3. The energy expended during the induction and centrifugal pumping of the internal flow, if properly conserved within the internal system, can be partly regained as jet-propulsive effect by efficient rejection from the tip nozzle. In the ideal case the motion of the internal flow (without heat) would not create any loss.

4. The loss of propeller efficiency associated with the internal flow increases with the pressure loss in the internal system.

5. For the propeller tested, more than one-half of the pressure available for forcing the internal flow through the propeller was required to overcome the pressure loss within the internal system.

6. The internal pressure loss coefficient  $\Delta p_f/q_N$  (which is proportional to skin friction and turbulence losses) increases with increasing rotational speed.

7. In calculating the internal flow characteristics, the assumption that the static pressure at the nozzle exit was equal to the atmospheric pressure in which the propeller was operating was found to be justified for the propeller tested.

Langley Memorial Aeronautical Laboratory  
National Advisory Committee for Aeronautics  
Langley Field, Va., May 7, 1946

## APPENDIX A

## SYMBOLS

$A_N$	total nozzle exit area, sq ft
$C_{D_N}$	nozzle external drag coefficient based on total nozzle area, $A_N$
$C_P$	power coefficient $\left(\frac{P}{\rho n^3 D^5}\right)$
$c_p$	specific heat of air, Btu/slug/°F ( $c_p = 7.73$ )
$C_T$	thrust coefficient $\left(\frac{T}{\rho n^2 D^4}\right)$
$D$	propeller diameter, ft
$D_N$	drag on the propeller blades caused by the presence of the nozzles, lb
$F_N$	force on propeller blades due to jet reaction at the nozzles, lb
$H_I$	heat contained in the internal flow entering the propeller, Btu/sec
$H_D$	heat dissipated through the propeller surface, Btu/sec
$J$	propeller advance ratio $V/nD$
$m$	mass flow through the internal system, slugs/sec
$m_c$	coefficient of internal-mass flow $\left(\frac{m}{\rho A_N n D}\right)$
$n$	propeller rotational speed, rps
$P$	power, ft-lb/sec

$p$	static pressure, lb/sq ft
$p_o$	static pressure in metering orifice, lb/sq ft
$p_a$	atmospheric pressure (barometric pressure), lb/sq ft
$\Delta p$	pressure change in metering orifice, lb/sq ft ( $\Delta p = p_a - p_o$ )
$\Delta p_A$	equivalent pressure available for moving the flow through the internal system, lb/sq ft
$\Delta p_f$	pressure loss across the internal-flow system, lb/sq ft
$\Delta p_R$	net pressure required to move the flow through the internal system, lb/sq ft
$Q$	torque, ft-lb
$q$	dynamic pressure, lb/sq ft $\left(\frac{1}{2}\rho v^2\right)$
$q_N$	dynamic pressure at the nozzle, lb/sq ft $\left(\frac{1}{2}\rho_N V_N^2\right)$
$r$	radius at any blade section, ft
$T$	propeller thrust, lb
$t$	static temperature of the air, °F abs.
$V$	velocity of advance, ft/sec
$V_N$	velocity of air leaving nozzle, ft/sec
$W$	resultant air velocity, ft/sec
$x$	fraction of propeller tip radius
$\alpha$	angle of attack, deg
$\beta$	blade angle, deg
$\epsilon$	nozzle effectiveness

$\eta$  propeller efficiency (without nozzles and internal flow)

$\eta_N$  nozzle propulsive efficiency

$\lambda$  the term  $1 + \frac{(nD)^2 [(\pi x)^2 + J^2]}{1556c_p t}$

$\tau$  the term  $\sqrt{\frac{(\pi x)^2 + J^2}{m_c^2}}$

$\rho$  mass density of air, slugs/cu ft

$\rho_N$  mass density of internal flow at the nozzle, slugs/cu ft

$\omega$  angular velocity, radians/sec

## APPENDIX B

## ELIMINATION OF DENSITY RATIO FROM EQUATION (26)

If the energy in the internal flow consumed by pressure loss appears as heat in the flow, if none of the heat is transferred from the flow, and if the static pressure at the nozzle is equal to that of the free-air stream, the air density at the nozzle can be evaluated in terms of the internal pressure loss and eliminated from equation (26).

The power that goes into heat in the internal flow is

$$\text{Energy per second} = \frac{m}{2} \left[ (\pi n D x)^2 + v^2 - v_N^2 \right]$$

and, since

$$v_N = m_c \left( \frac{\rho}{\rho_N} \right) n D$$

$$\text{Energy per second} = \frac{m(nD)^2}{2} \left[ (\pi x)^2 + J^2 - \left( m_c \frac{\rho}{\rho_N} \right)^2 \right]$$

From equation (27)

$$\left( m_c \frac{\rho}{\rho_N} \right)^2 = \frac{(\pi x)^2 + J^2}{\frac{\Delta p_f}{q_N} + 1}$$

Therefore

$$\text{Energy per second} = \frac{m(nD)^2}{2} \left[ (\pi x)^2 + J^2 \right] \left( 1 - \frac{1}{\frac{\Delta p_f}{q_N} + 1} \right)$$

foot-pounds/second

Expressed in heat units the foregoing rate of heat generation becomes

$$778 \text{ Btu per second} = \frac{m(nD)^2}{2} \left[ (\pi x)^2 + J^2 \right] \left( \frac{\frac{\Delta p_f}{q_N}}{\frac{\Delta p_f}{q_N} + 1} \right)$$

The static temperature rise  $\Delta t$  resulting from the heat generated by losses in the internal flow is

$$\Delta t = \frac{(\text{Btu per second})}{mc_p}$$

where  $c_p = 7.73$  is the specific heat of air in Btu per slug per  $^{\circ}\text{F}$ . The temperature rise thus becomes

$$\Delta t = \frac{(nD)^2}{1556c_p} \left[ (\pi x)^2 + J^2 \right] \frac{\frac{\Delta p_f}{q_N}}{\frac{\Delta p_f}{q_N} + 1} \quad (37)$$

If equal static pressures are assumed for the external and internal flows, the ratio of free-stream air density to density of the internal flow at the nozzle is inverse to the ratio of the absolute temperatures

$$\frac{\rho}{\rho_N} = 1 + \frac{\Delta t}{t}$$

where  $t$  is the free-stream absolute temperature. If

equation (37) is used to express the temperature rise due to internal losses, the density ratio becomes

$$\frac{\rho}{\rho_N} = 1 + \frac{(nD)^2}{1556c_p t} \left[ (\pi x)^2 + J^2 \right] \frac{\frac{\Delta p_f}{q_N}}{\frac{\Delta p_f}{q_N} + 1}$$

Equation (27) can be rewritten:

$$\frac{\rho}{\rho_N} = \sqrt{\frac{(\pi x)^2 + J^2}{\left(\frac{\Delta p_f}{q_N} + 1\right) m_c^2}}$$

When the two foregoing expressions for density ratio are equated, the resulting expression relates the internal pressure loss to advance ratio, rotational speed, mass-flow coefficient, and free-stream temperature (quantities which were measured during the tests reported in reference 1):

$$\sqrt{\frac{(\pi x)^2 + J^2}{\left(\frac{\Delta p_f}{q_N} + 1\right) m_c^2}} = 1 + \frac{(nD)^2}{1556c_p t} \left( \frac{\frac{\Delta p_f}{q_N}}{\frac{\Delta p_f}{q_N} + 1} \right) \left[ (\pi x)^2 + J^2 \right]$$

(equation (33))

Equation (33) can be solved for an explicit expression of the internal pressure loss, as follows:

$$\frac{\Delta p_f}{q_N} = \frac{\tau^2 - 2\lambda}{2\lambda^2} \pm \frac{\tau}{\lambda} \sqrt{1 - \frac{1}{\lambda} + \frac{\tau^2}{4\lambda^2}}$$

where

$$\tau = \sqrt{\frac{(\pi x)^2 + J^2}{m_c^2}}$$

$$\lambda = \left\{ 1 + \frac{(nD)^2 [(\pi x)^2 + J^2]}{1556 c_p t} \right\}$$

## APPENDIX C

## CALCULATION OF AIR DENSITY AT THE NOZZLE

If, as has been assumed throughout this analysis, the static pressure at the nozzle is the same as that of the atmosphere in which the airplane is flying, the relation between air density and temperature is

$$\frac{\rho_N}{\rho} = \frac{t}{t + \Delta t}$$

where  $t$  is the ambient temperature and  $\Delta t$  is the temperature difference between air at the nozzle and atmospheric air. The temperature elevation due to residual heat in the heated internal flow is

$$\frac{H_I - H_D}{mc_p}$$

where  $H_I$  is the rate (Btu per second) at which heat contained in the internal flow enters the propeller and  $H_D$  the rate at which heat is dissipated through the propeller blade surface for de-icing. The temperature rise due to the heat generated by the internal pressure loss is shown in equation (37) to be

$$\frac{(nD)^2}{1556c_p} \left[ (\pi x)^2 + J^2 \right] \frac{\frac{\Delta p_f}{q_N}}{\frac{\Delta p_f}{q_N} + 1}$$

The temperature elevation of the internal flow at the nozzle due to added heat and internal losses is

$$\Delta t = \frac{H_I - H_D}{mc_p} + \frac{(nD)^2}{1556c_p} \left[ (\pi x)^2 + J^2 \right] \frac{\frac{\Delta p_f}{q_N}}{\frac{\Delta p_f}{q_N} + 1}$$

Equation (28) gives the relation

$$\frac{\frac{\Delta p_f}{q_N}}{\frac{\Delta p_f}{q_N} + 1} = \frac{\Delta p_f}{\Delta p_A}$$

Combining the two foregoing equations and using equation (24) to express the pressure available  $\Delta p_A$  gives the expression for the total temperature rise

$$\Delta t = \frac{H_I - H_D}{mc_p} + \frac{\Delta p_f}{778c_p \rho_N}$$

The air density at the nozzle, therefore, becomes

$$\rho_N = \rho \left( \frac{t}{t + \frac{H_I - H_D}{mc_p} + \frac{\Delta p_f}{778c_p \rho_N}} \right)$$

Transposing gives

$$\rho_N \left( t + \frac{H_I - H_D}{mc_p} \right) + \frac{\Delta p_f}{778c_p} = t\rho$$

and

$$\rho_N = \left( \frac{\rho - \frac{\Delta p_f}{778c_p t}}{1 + \frac{H_I - H_D}{mc_p t}} \right) \quad (\text{equation (31)})$$

## REFERENCES

1. Corson, Blake W., Jr., and Maynard, Julian D.: Investigation of the Effect of a Tip Modification and Thermal De-Icing Air Flow on Propeller Performance. NACA TN No. 1111, 1946.
2. Kantrowitz, Arthur: Aerodynamic Heating and the Deflection of Drops by an Obstacle in an Air Stream in Relation to Aircraft Icing. NACA TN No. 779, 1940.
3. Rodert, Lewis A.: The Effects of Aerodynamic Heating on Ice Formations on Airplane Propellers. NACA TN No. 799, 1941.
4. Pye, D. R.: The Internal Combustion Engine. Vol. II. The Aero-Engine. Clarendon Press (Oxford), 1934, p. 264.
5. Becker, John V., and Baals, Donald D.: The Aerodynamic Effects of Heat and Compressibility in the Internal Flow Systems of Aircraft. NACA ACR, Sept. 1942.

TABLE I  
 COMPUTATION OF EFFICIENCY LOSS DUE TO  
 NOZZLE DRAG AT PEAK EFFICIENCY

$$\left[ A_N = 0.00903 \text{ sq. ft.}; D = 12.208 \text{ ft.}; x = 0.95; \right. \\ \left. C_{D_N} = 1.28 \text{ (assumed)} \right]$$

$\beta$ at 42-inch radius  (deg)	$J$  (a)	$\eta$ (normal propeller)  (a)	$C_p$ (normal propeller)  (b)	$-\Delta\eta$ (computed from equation (7))	$\eta$ (tip nozzle without flow) (c)	$-\Delta\eta$ (measured)
24.9	0.73	0.812	0.031	0.0298	0.782	0.030
29.9	.95	.837	.045	.0226	.820	.017
35.3	1.15	.845	.067	.0164	.834	.011
40.1	1.38	.840	.096	.0125	.830	.010
44.9	1.63	.835	.131	.0099	.824	.011
50.3	1.91	.826	.170	.0089	.817	.009
55.4	2.30	.808	.227	.0080	.798	.010
60.5	2.77	.779	.293	.0079	.773	.006

<sup>a</sup>Figure 14, reference 1.

<sup>b</sup>Figure 13, reference 1.

<sup>c</sup>Figure 17, reference 1.

NATIONAL ADVISORY  
 COMMITTEE FOR AERONAUTICS

TABLE II  
 EFFICIENCY LOSS AT PEAK EFFICIENCY DUE TO INTERNAL FLOW  
 [  $A_N = 0.00903$  sq ft;  $D = 12.208$ ;  $x = 0.95$ ;  $\epsilon = 0.75$  (assumed) ]

$\beta$ at 42-inch radius (deg)	J (a)	$\eta$ (tips open, no flow) (a)	$C_p$ (tips open, no flow) (b)	$m_c$ (propel- ler with internal flow) (c)	$\frac{P}{P_N}$ (from fig. 8)	$-\Delta\eta$ (computed from equation (20))	$\eta$ (propel- ler with internal flow) (d)	$-\Delta\eta$ (measured)
24.9	0.730	0.784	0.0315	1.923	1.061	0.014	0.779	0.005
29.9	.920	.822	.0460	1.949	1.061	.011	.801	.021
35.3	1.140	.836	.0680	1.996	1.061	.008	.821	.015
40.1	1.350	.832	.0952	2.048	1.061	.006	.823	.009
44.9	1.650	.826	.1220	2.140	1.061	.005	.818	.008
50.3	1.800	.822	.1883	2.294	1.047	.004	.815	.007
55.4	2.300	.797	.2305	2.507	1.047	.004	.795	.002
60.5	2.600	.787	.3065	2.689	1.038	.004	.785	.002

a Figure 17, reference 1.  
 b Figure 16, reference 1.  
 c Figure 27, reference 1.  
 d Figure 23, reference 1.

NATIONAL ADVISORY  
 COMMITTEE FOR AERONAUTICS

TABLE III  
 EFFICIENCY LOSS AT PEAK EFFICIENCY DUE TO COMBINED  
 EFFECT OF NOZZLE DRAG AND INTERVAL FLOW

$[A_N = 0.00903 \text{ sq ft}; D = 12.208; x = 0.95;$   
 $C_{D_N} = 1.28 \text{ (assumed); } \epsilon = 0.75 \text{ (assumed)}]$

$\beta$ at 42-inch radius (deg)	J (a)	$\eta$ (normal propel- ler) (a)	$C_p$ (normal propel- ler) (b)	$m_c$ (propel- ler with interval flow) (c)	$\frac{p}{p_N}$ (from fig 8)	$-\Delta\eta$ (computed from equa- tion (21))	$\eta$ (propel- ler with interval flow) (d)	$-\Delta\eta$ (measured)
24.9	0.73	0.812	0.031	1.923	1.061	0.045	0.779	0.033
29.9	.95	.837	.045	1.951	1.061	.034	.798	.039
35.3	1.15	.845	.067	1.998	1.061	.024	.820	.025
40.1	1.38	.840	.096	2.054	1.061	.019	.820	.020
44.9	1.63	.835	.131	2.136	1.061	.015	.820	.015
50.3	1.91	.826	.170	2.332	1.047	.013	.812	.014
55.4	2.30	.808	.227	2.507	1.047	.012	.779	.009
60.5	2.77	.779	.293	2.760	1.038	.012	.772	.007

aFigure 14, reference 1.  
 bFigure 13, reference 1.  
 cFigure 27, reference 1.  
 dFigure 23, reference 1.

NATIONAL ADVISORY  
 COMMITTEE FOR AERONAUTICS

TABLE IV  
COMPUTATION OF INTERNAL PRESSURE LOSS

$\beta$ at 42-inch radius (deg)	Propel- ler speed (rpm)	J	$m_c$	t (°F abs.)	$\frac{\Delta p_f}{q_N}$	$\frac{\rho_N}{\rho}$	Nominal a (deg)
Constant propeller speed (reference 1, figs. 27 and 28)							
29.9	1450	0.704	1.817	554	1.47	0.932	5.01
29.9	1450	1.232	1.917	549	1.43	.926	-3.86
35.3	1450	1.065	1.861	537	1.49	.927	3.98
35.3	1450	1.494	1.990	537	1.39	.922	-2.93
24.9	1240	.562	1.923	535	1.27	.954	2.62
24.9	1240	1.000	1.951	536	1.33	.946	-5.25
29.9	1240	.695	1.939	554	1.27	.954	5.17
29.9	1240	1.219	1.992	553	1.34	.946	-3.95
35.3	1240	.788	1.956	545	1.25	.951	8.89
35.3	1240	1.482	2.067	540	1.30	.941	-2.74
40.1	1240	1.236	2.023	528	1.28	.946	5.97
40.1	1240	1.782	2.162	527	1.27	.937	-2.38
44.9	1240	1.669	2.145	543	1.25	.941	4.05
44.9	1240	2.108	2.292	542	1.21	.933	-1.97
50.3	1000	1.793	2.289	532	1.13	.960	7.67
50.3	1000	2.565	2.574	527	1.10	.948	-2.02
55.4	1000	2.407	2.549	533	1.06	.954	4.87
55.4	1000	3.093	2.850	531	1.02	.943	-2.27
60.5	800	2.590	2.689	537	1.03	.970	7.91
60.5	800	3.795	3.267	531	.99	.955	-2.97
Constant J, variable propeller speed (reference 1, fig. 29)							
24.9	1400	0.711	1.853	536	1.40	0.936	-0.12
29.9	600	.967	2.129	555	1.12	.988	.32
35.3	1500	1.330	1.915	534	1.45	.917	-.35
40.1	1300	1.657	2.103	527	1.29	.933	-.58
40.1	1100	1.638	2.167	530	1.23	.951	-.30
44.9	300	2.027	2.477	554	1.10	.995	-.92
44.9	800	2.040	2.347	550	1.24	.972	-1.09
50.3	500	2.442	2.623	539	1.11	.988	-.63
50.3	700	2.421	2.567	538	1.13	.975	-.39
50.3	900	2.448	2.543	532	1.12	.959	-.70
55.4	500	2.954	2.837	548	1.13	.986	-1.45
55.4	1000	2.954	2.778	532	1.05	.947	-1.45
60.5	300	3.446	3.195	549	1.01	.994	-.25
60.5	400	3.482	3.114	549	1.12	.989	-.56
60.5	600	3.514	3.118	541	1.08	.976	-.80

TABLE IV - Concluded

## COMPUTATION OF INTERNAL PRESSURE LOSS - Concluded

$\beta$ at 1/2-inch radius (deg)	V (ft/sec)	$\frac{m_c}{J}$		t (°F abs.)	$\frac{\Delta p_f}{q_N}$	$\frac{\rho_N}{\rho}$	Nominal $\alpha$ (deg)
Propeller feathered, propeller speed = 0 (reference 1, fig. 30)							
88.7	131.7	0.743	-----	535	0.816	1.000	-12.9
88.7	297.9	.708	-----	534	.967	.993	-12.9
88.7	574.8	.708	-----	518	.898	.976	-12.9

NATIONAL ADVISORY  
COMMITTEE FOR AERONAUTICS

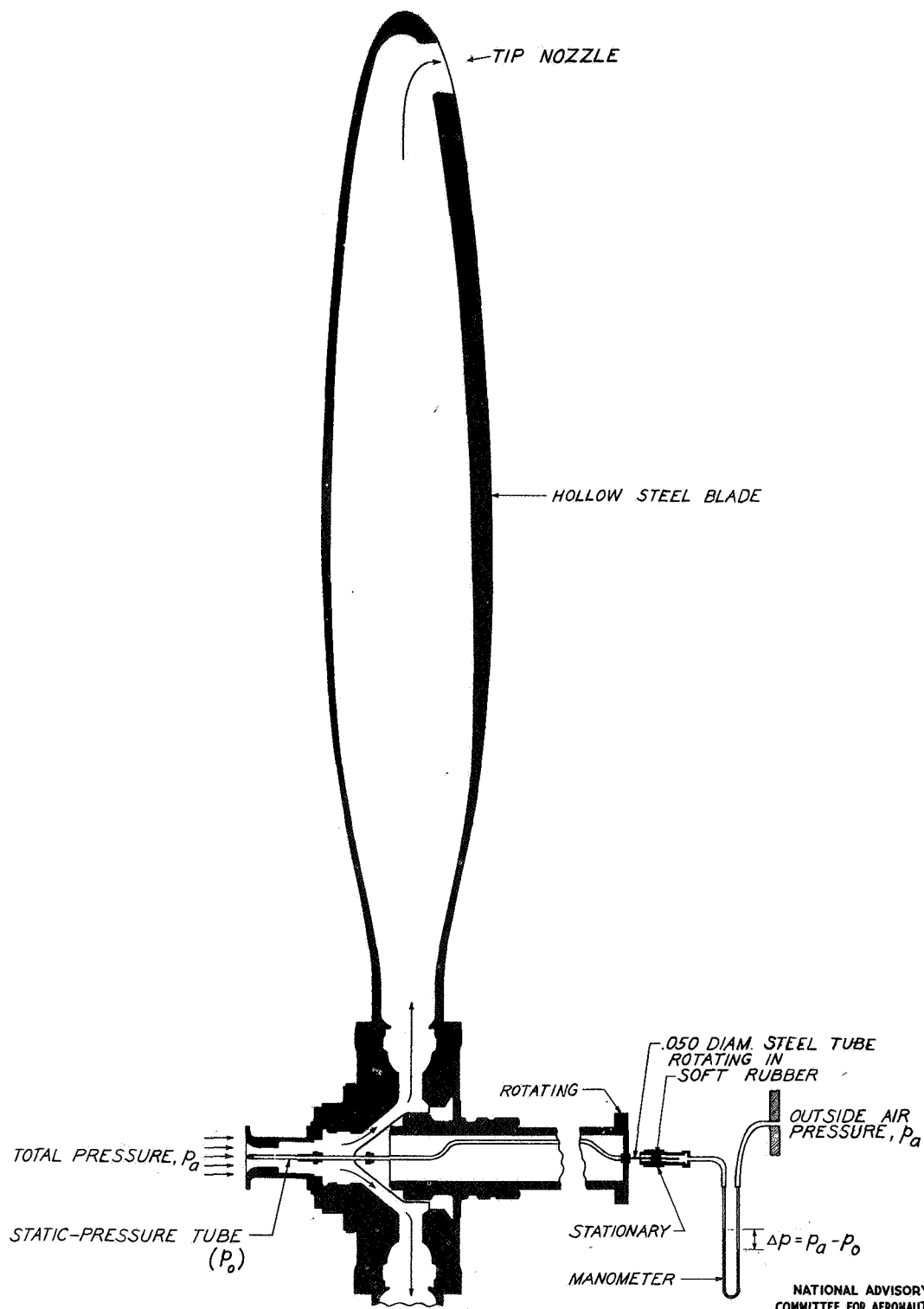
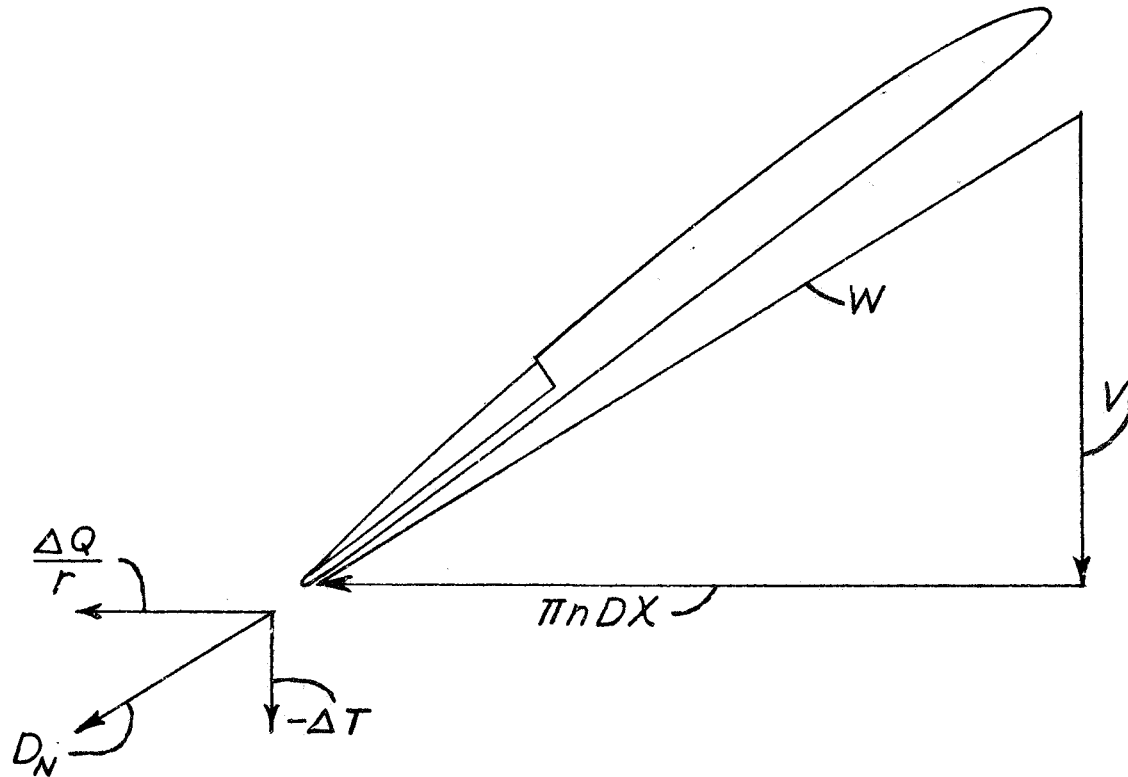
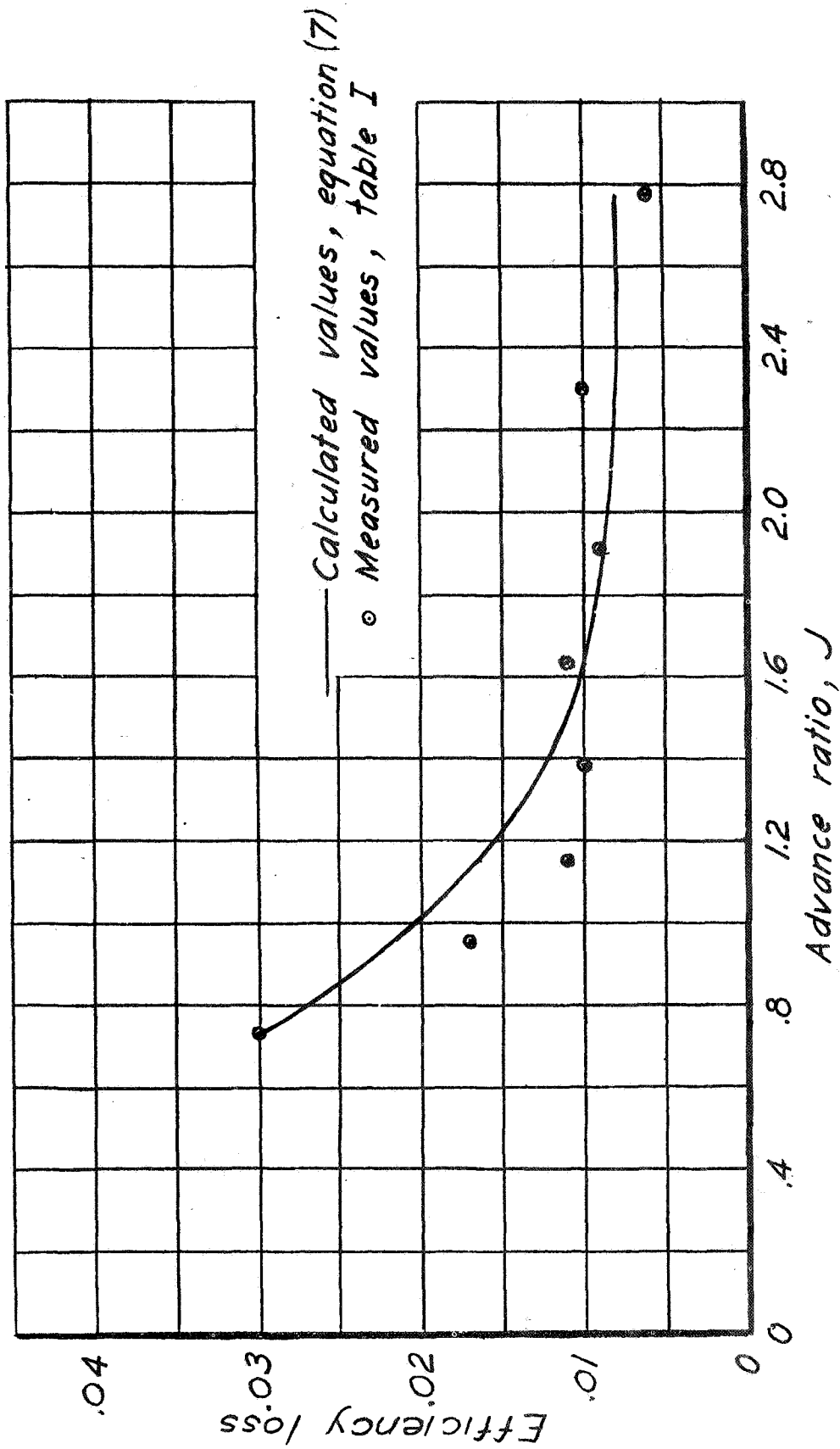


FIGURE 1.— PATH OF INTERNAL FLOW THROUGH THE PROPELLER AND THE INTERNAL-MASS-FLOW METER.



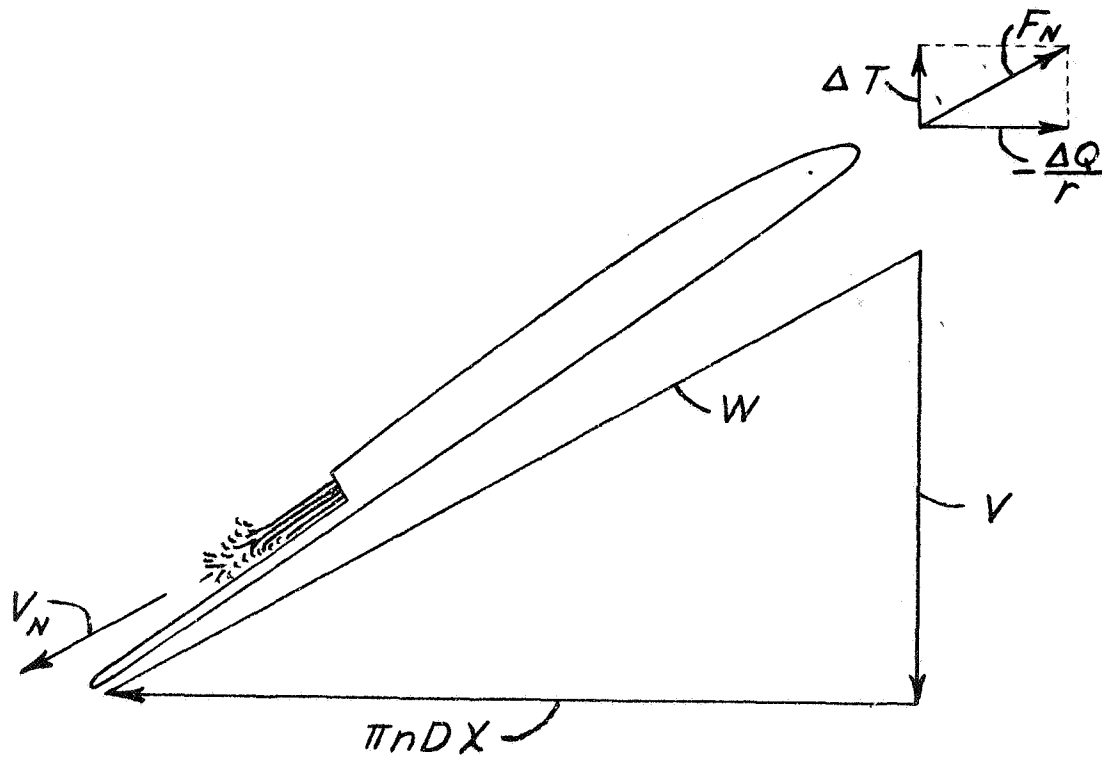
NATIONAL ADVISORY  
COMMITTEE FOR AERONAUTICS

Figure 2.- A diagram of velocities and forces associated with the nozzle drag.



NATIONAL ADVISORY  
COMMITTEE FOR AERONAUTICS

Figure 3. - Propeller efficiency loss at peak efficiency due to drag of nozzles without internal flow.



NATIONAL ADVISORY  
COMMITTEE FOR AERONAUTICS

Figure 4.- A diagram of the velocities and forces associated with the jet propulsion due to flow from the nozzle.

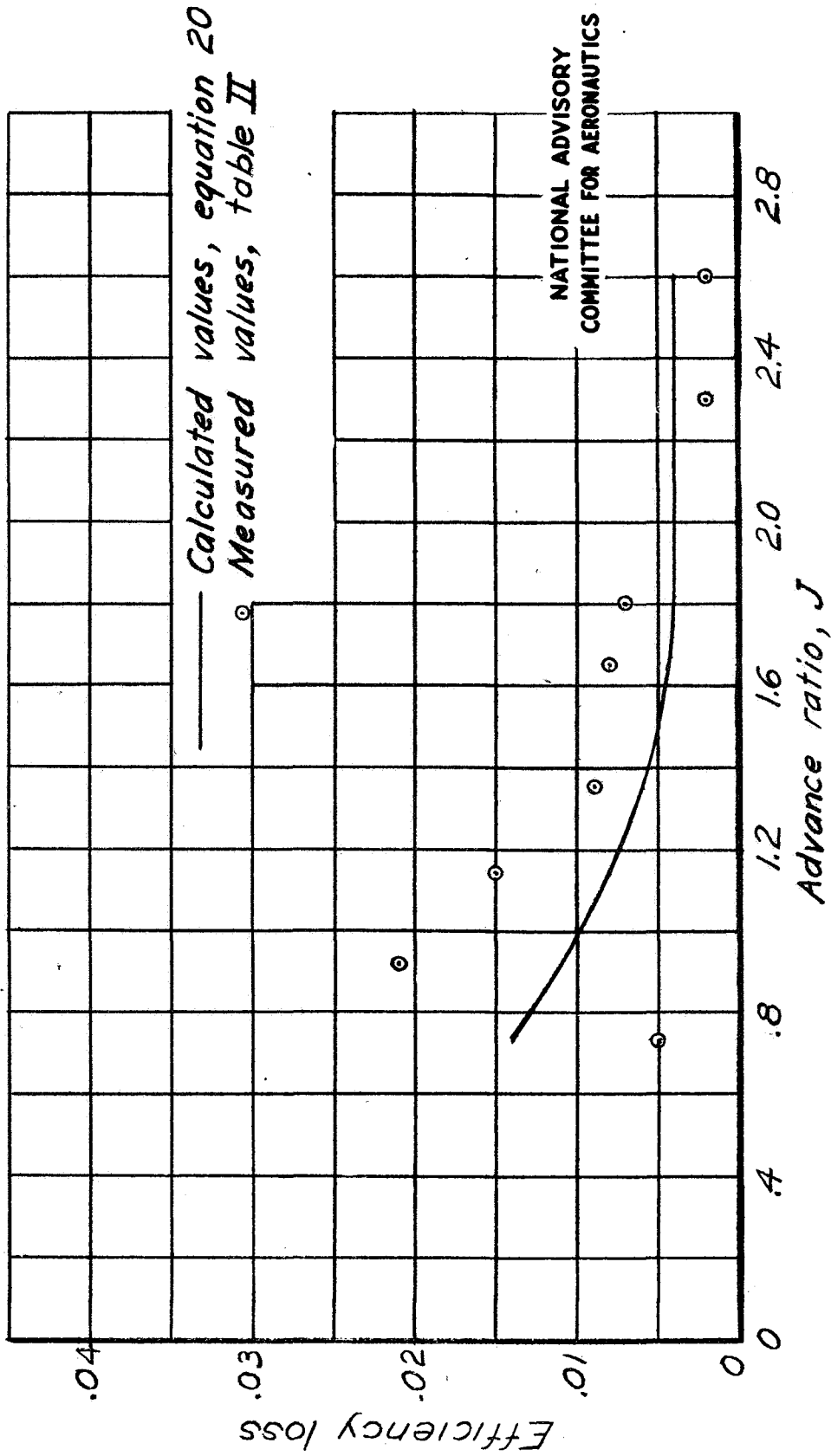


Figure 5. - Propeller efficiency loss at peak efficiency due to internal flow.

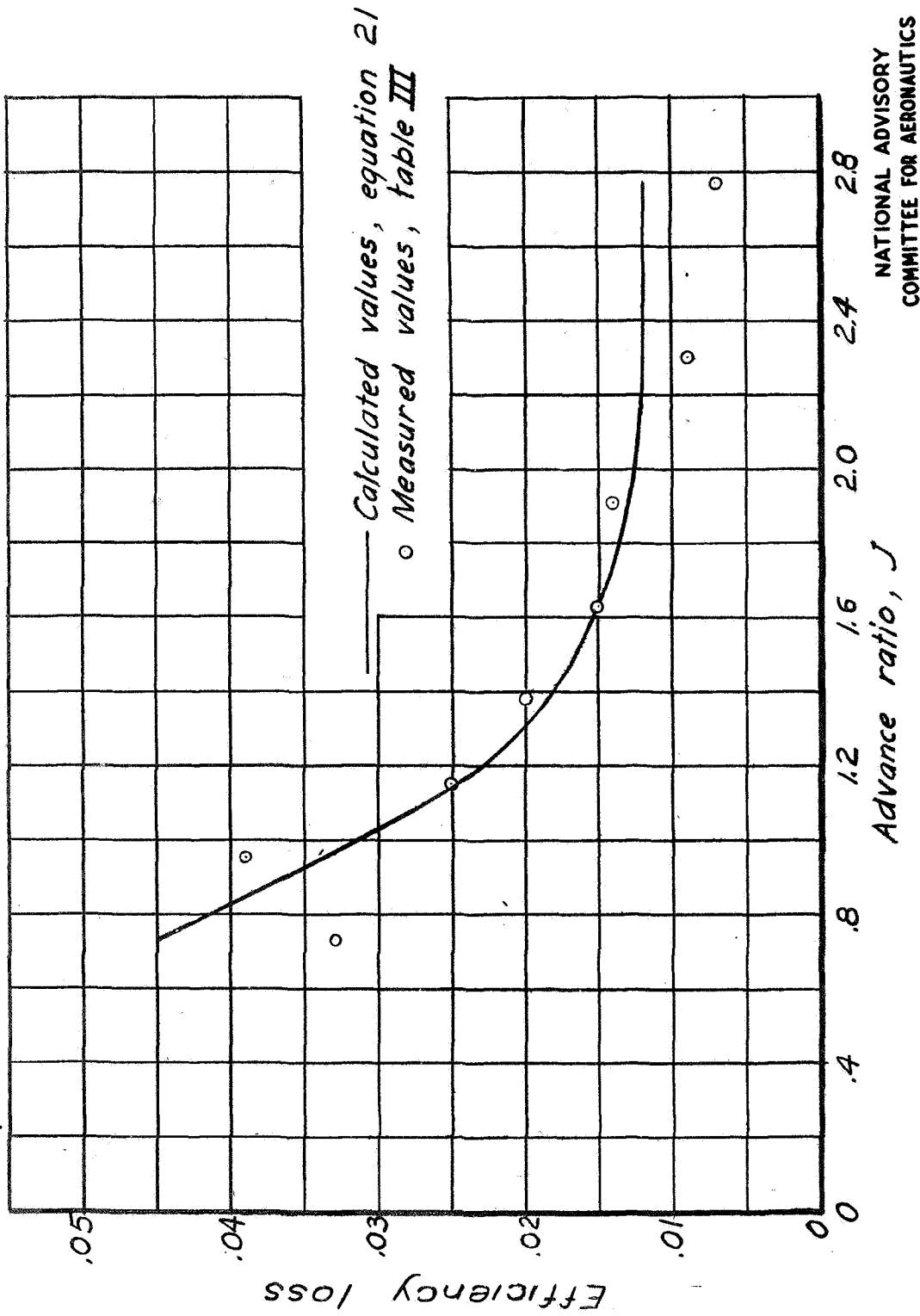


Figure 6.- Propeller efficiency loss at peak efficiency due to combined effect of nozzle drag and internal flow.

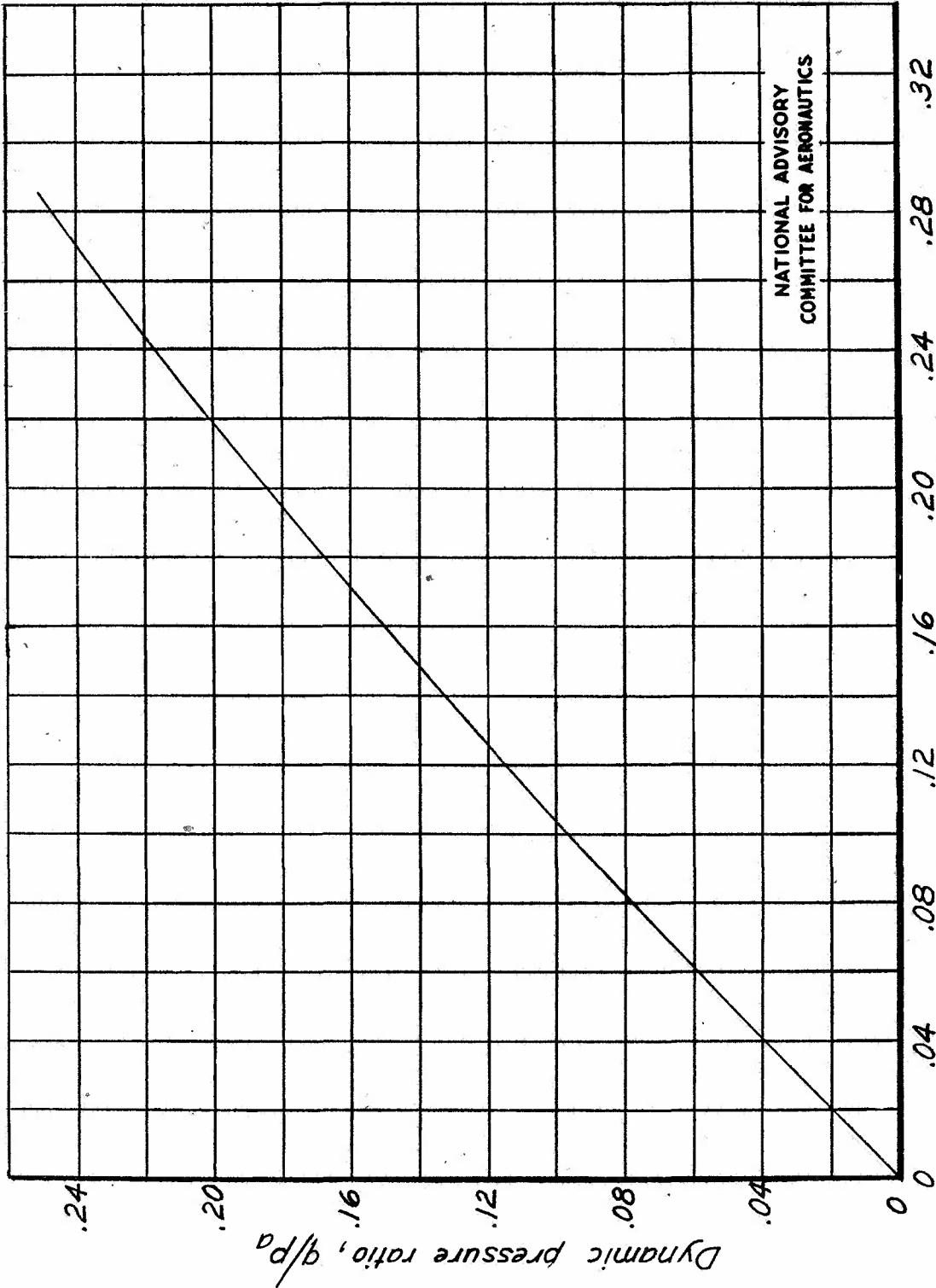


Figure 7.- Variation of dynamic pressure ratio with impact pressure ratio.

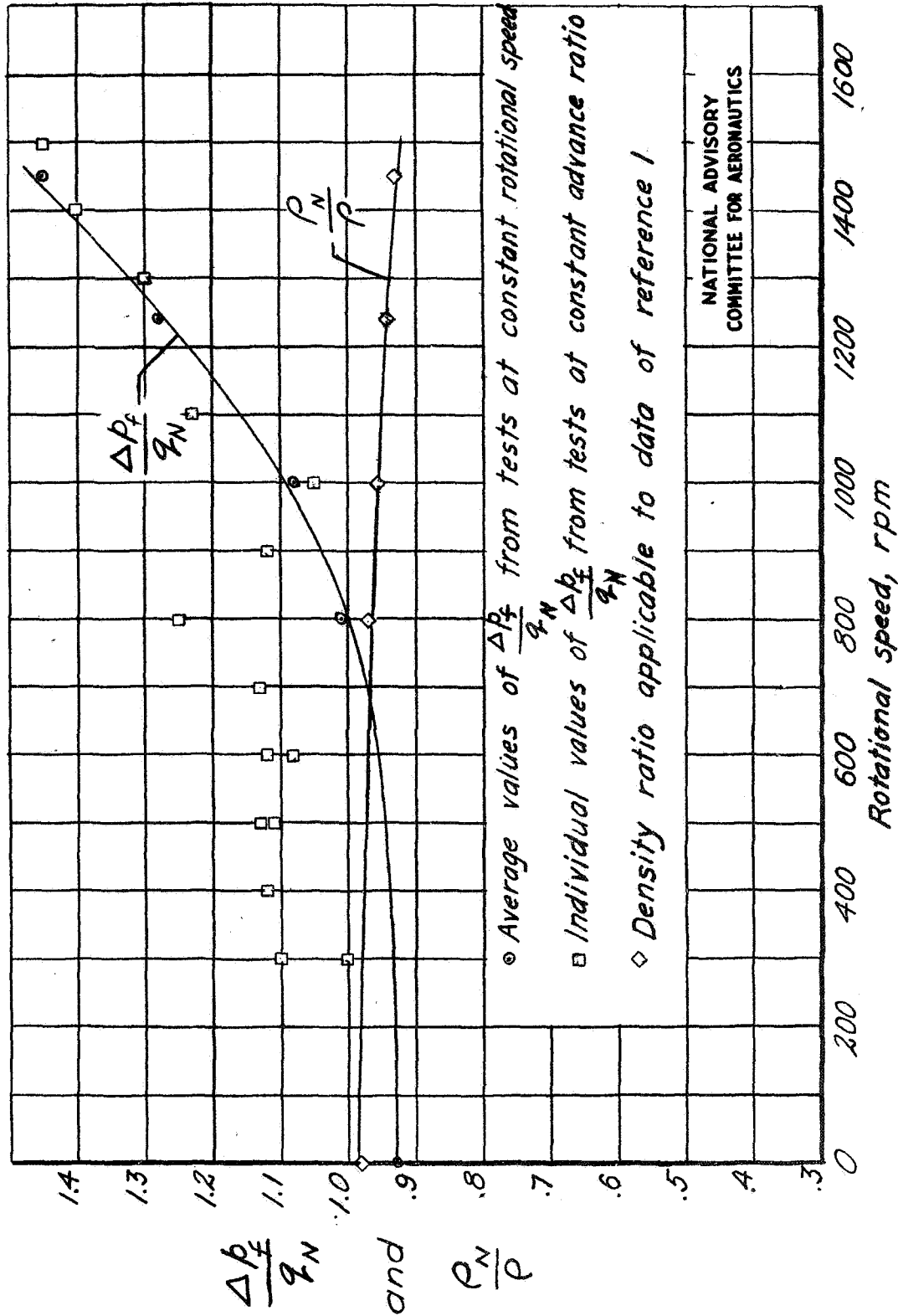


Figure 8.- Variation of internal pressure loss and density ratio with rotational speed.

TITLE: Analysis of Propeller Efficiency Losses Associated with Heated Air Thermal  
De-icing  
AUTHOR(S): Corson, Blake W.  
ORIGINATING AGENCY: National Advisory Committee for Aeronautics, Washington, D. C.  
PUBLISHED BY: Same

ATI- 6111

EDITION  
None

ORIG. AGENCY NO.  
TN-1112

PUBLISHING AGENCY NO.

DATE	DOC. CLASS.	COUNTRY	LANGUAGE	PAGES	ILLUSTRATIONS
July '46	Unclass.	U.S.	English	54	tables, graphs, drawing

ABSTRACT:

Analysis is made of loss of efficiency associated with heated-air thermal de-icing propeller both with and without internal flow. For available data, measured efficiency losses are compared with calculated losses and agreement is found to be within experimental accuracy of data. Method presented may be used with reasonable accuracy to determine net change in propeller efficiency caused by combined effects of nozzle and internal flow if characteristics of propeller without nozzles are known.

DISTRIBUTION: Request copies of this report only from Originating Agency

DIVISION: Propellers (11)  
SECTION: Ice Control (5)

SUBJECT HEADINGS: Ice formation - Prevention (50201);  
Propellers - Performance (75478.28); Propellers - Aero-  
dynamics - Anti-icing effect (75478.115); Propellers -  
Anti - Icing, Hot air (75478.158)

ATI SHEET NO.:

Air Documents Division, Intelligence Department  
Air Materiel Command

AIR TECHNICAL INDEX

Wright-Patterson Air Force Base  
Dayton, Ohio